Dual Surface-Functionalized Janus Nanocomposites of Polystyrene/Fe_3O_4@SiO_2 for Simultaneous Tumor Cell Targeting and Stimulus-Induced Drug Release

Feng Wang, Giovanni M. Pauletti, Juntao Wang, Jiaming Zhang, Rodney C. Ewing, Yilong Wang, and Donglu Shi**

One of the critical challenges in medical diagnosis and therapy using nanotechnology is the assembly of multiple components in a multifunctional delivery system. This includes functionalities that can be structurally and chemically tailored in a nanocarrier for multi-modality imaging, cell targeting, drug storage, and controlled drug release. Development of these complex systems primarily utilizes existing basic nanosystems, such as carbon nanotubes, graphene, iron oxides, silica, quantum dots, and polymeric nanomaterials. Extensive attempts have been made to design, synthesize, and assemble some of these major components described above, for diagnostic and therapeutic delivery systems. Most of the approaches center on surface functionalization with drugs,[1] biotechnology-derived molecules, including DNA,[2] RNA,[3] peptides,[4] and antibodies,[5] and imaging agents such as quantum dots.[6] One of the major limitations of this approach is the single surface structure of the nanosystem. To date, nanoparticles represent the most widely used carrier system for multifunctional drug delivery applications.[7] These structures normally assume a symmetrical, spherical or tubular geometry with limited surface available for attachment of multiple components. Frequently, multifunctional conjugates on a single carrier interact with each other leading to undesired adverse effects. The design and assembly of a symmetrical, single surface carrier is further complicated by unfavorable structural and chemical arrangements of these functional components. It is, therefore, critical to develop multi-surface nanostructures for assembly of a variety of components using a clinically acceptable drug delivery platform that can best utilize the intrinsic properties of the nanomaterials.

Janus nanoparticles possess multiple surface structures that are anisotropic in shape, composition, and surface chemistry.[8] Their structural asymmetry is ideally suited for multiple-component conjugations on a single-particle system.[9] More importantly, functionally distinct surfaces of the Janus particle can be used to selectively conjugate specific chemical moieties for cell targeting, non-invasive imaging, and/or therapeutic intervention.[10] These characteristics of the Janus nanoparticles render them truly "multifunctional entities".[11] A variety of fabrication methods[12] have been reported to synthesize Janus nanoparticles for applications such as surfactants,[13] magnetic-fluorescent display or imaging,[14] catalysts,[15] and drug delivery.[16] However, only a few studies explored the potential of these chemically different surfaces on Janus nanoparticles for multifunctional drug delivery applications that simultaneous achieve cell targeting and stimulus-induced drug release.

In this study, super-paramagnetic Janus nanocomposites (SJNCs) of polystyrene/Fe_3O_4@SiO_2 were developed using a combined process of miniemulsion and sol–gel reaction.[17] The structure of SJNCs is schematically illustrated in **Figure 1**. The SJNCs are composed of a polystyrene (PS) core and a half silica shell with iron oxide nanoparticles embedded in its matrix. Conceptionally, the nanocomposite comprises two unique surfaces suitable for selective chemical modification using different functional groups. In contrast to previous approaches used to prepare Janus nanoparticles,[18] this communication outlines for the first time a one-pot facile synthesis that successfully yields a Janus structure with desired dual functionalities for drug delivery applications.

To engineer chemically distinct surface properties required for simultaneous cell targeting and stimulus-induced drug release without chemical or steric interference, the PS matrix was surface-decorated with carboxyl groups. Tumor cell targeting was attempted by the conjugation of folic acid (FA) to the PS surface using a bis-amine linker (Figure 1). The antitumor agent doxorubicin (DOX) was immobilized to the silica shell via a pH-sensitive hydrazone bond facilitating stimulus-induced drug release. It was hypothesized that this design enables efficient interaction of the drug-loaded Janus structure with cancer cells that overexpress folate receptors.[19] Following receptor mediated endocytosis, exposure to the acidic

F. Wang, Prof. D. Shi
Materials Science and Engineering Program
University of Cincinnati
Cincinnati, OH 45221, USA
E-mail: shid@ucmail.uc.edu
Prof. G. M. Pauletti
James L. Winkle College of Pharmacy
University of Cincinnati
Cincinnati, OH 45267, USA
J. Wang, Dr. Y. Wang, Prof. D. Shi
Institute for Biomedical Engineering & Nano Science
Tongji University School of Medicine
Shanghai 200092, China
E-mail: yilongwang@tongji.edu.cn
Dr. J. Zhang, Prof. R. C. Ewing
Departments of Earth & Environmental Sciences
Nuclear Engineering & Radiological Sciences
and Materials Science & Engineering
University of Michigan
Ann Arbor, MI 48109-1005, USA

DOI: 10.1002/adma.201301376

ADVANCED MATERIALS
www.advmat.de

www.MaterialsViews.com

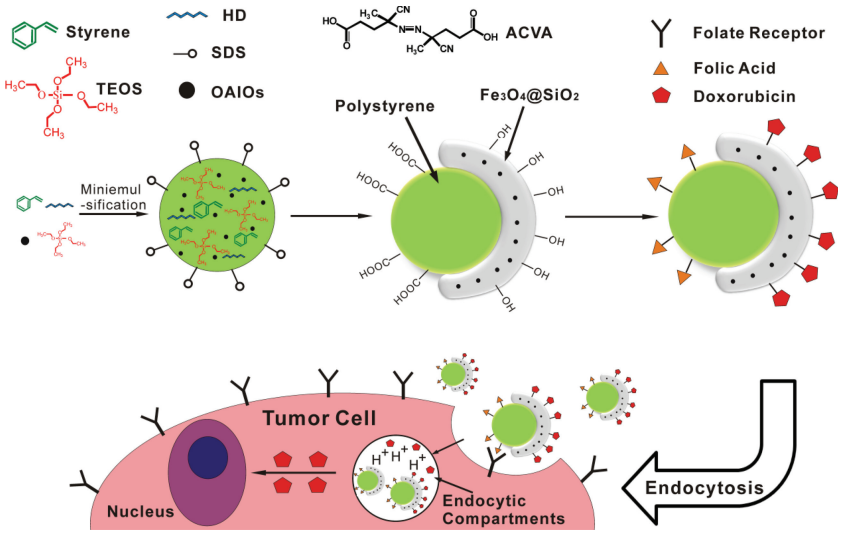

Figure 1. Schematic diagram illustrating the synthesis of polystyrene/Fe_3O_4@SiO_2 superparamagnetic Janus nanocomposites (SJNCs) and the proposed mechanisms for tumor cell targeting and stimulus-induced drug release.

endosomal compartment (pH 4.5–6.5)[20] is predicted to hydrolyze the pH-sensitive linker releasing pharmacologically active DOX. The therapeutic advantage of this novel nanostructure is that only tumor cells will be exposed to high concentrations of the cytotoxic DOX because of chemical stability of the hydrazone bond during bloodstream circulation at pH 7.4. Consequently, patients are expected to suffer less from side effects that are commonly associated with the systemic circulation of free DOX. Furthermore, incorporation of iron oxide nanoparticles allows non-invasive in vivo imaging using MRI, magnetic targeting, and generation of magnetically-induced hyperthermia that sensitizes tumor cells to cytotoxic drugs.[21] Thus, the Janus nanosystem is an ideal platform for developing versatile functionalities in biomedical applications.

SJNCs were synthesized using a one-pot miniemulsion process similar to the method reported in one of our earlier studies.[22] Briefly, styrene monomer, tetraethoxysilane, hexadecane, and oleic acid-functionalized iron oxides were mixed for miniemulsification process to form an oil-in-water miniemulsion system with sodium dodecyl sulfate as stabilizer. 4,4′-Azobis(4-cyanovaleric acid) was used as polymerization initiator that simultaneously allowed introduction of carboxyl groups on the PS surface. As shown in the scanning transmission electron microscopic (STEM) and transmission electron microscopic (TEM) images (**Figure 2**A,B), the dual-functionalized SJNCs have a PS core of ≈200 nm and a silica half shell with the thickness of around 100 nm. Fe_3O_4 nanoparticles of ≈10 nm are found to be dispersed and embedded in the matrix of the silica half shell. Physical stability of these Janus particles, following incubation for 6 days in buffer solutions ranging from pH 5–9, was confirmed (data not shown). Dynamic light scattering (DLS) data (see Supporting Information,

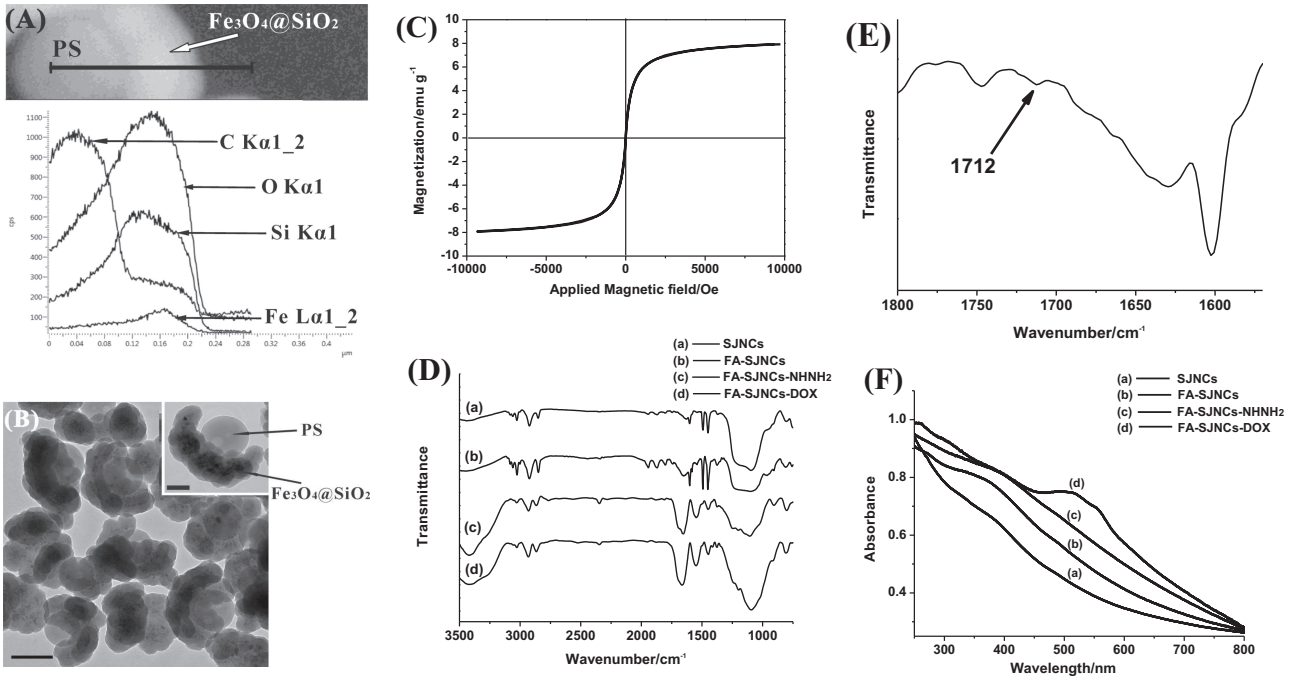

Figure 2. A) Elemental mapping of an individual SJNC. B) TEM image of SJNCs, the scale bar is 200 nm; inset: the SJNS image at higher magnification, the scale bar is 100 nm. C) the magnetization curve of SJNCs. D) FTIR spectra of a) SJNCs, b) FA-SJNCs, c) FA-SJNCs-$NHNH_2$, and d) FA-SJNCs-DOX. E) Magnified FTIR spectra of SJNCs. F) UV–vis spectra of: a) SJNCs, b) FA-SJNCs, c) FA-SJNCs-$NHNH_2$, and d) FA-SJNCs-DOX.

Figure S1) revealed a mean fully-hydrated particle size of 313 nm with a poly dispersity index (PDI) of 0.090. Elemental mapping (Figure 2A) confirmed a core predominantly composed of carbon while the half shell contains iron, silicon, and oxygen. The small peak at 1712 cm^{-1} in the FTIR spectra of SJNCs (Figure 2E) indicates the presence of carboxyl groups. According to the TG analysis (see Supporting Information, Figure S2), the polystyrene accounts for 14.2 wt.% of the nanocomposites. The SJNCs have a good magnetic response with a saturated magnetization at 8 emu g^{-1} (Figure 2C). The magnetic property of the composite can be used for the potential applications in MRI, magnetic targeting, and hyperthermia.

Carbodiimide-mediated coupling reaction was used to modify the PS surface with folic acid (FA). First, folic acid was linked to the poly(ethylene glycol) bis-amine spacer. Then the as-synthesized FA-PEG-NH_2 was conjugated to the PS surface. The UV-Vis spectrum shown in Figure 2F suggests successful surface immobilization of FA as evident by the characteristic shoulder around λ = 363 nm in the SJNCs curve after modification.[23] To couple DOX onto the silica surface, a silane-hydrazide crosslinker was synthesized by reacting 3-(triethoxysilyl)propyl isocyanate with adipic acid dihydrazide. After silica surface was modified with this crosslinker, DOX was covalently attached via formation of a hydrazone bond. The reaction scheme is illustrated in Figure S3, Supporting Information, in supporting information. DOX-containing SJNCs exhibit a broad shoulder in the UV-Vis spectrum, with the maximum absorption around λ = 517 nm that is distinct from the spectrum of the hydrazide-modified SJNCs. This peak deviates from the characteristic absorption maximum of free DOX around λ = 480 nm, most likely due to covalent immobilization.[24] On average, DOX loading was found to be 2.08 ± 0.2% (w/w).

Therapeutically required release of DOX from the Janus structure was predicted to be accelerated under acidic conditions in the endosome due to acid-catalyzed hydrolysis of the hydrazone linker. The in vitro drug release profiles shown in **Figure 3**A demonstrate that initial DOX release is four-fold faster at pH 5.0 than at pH 7.4. More importantly, the total amount of DOX released from these new Janus particles significantly increased under acidic conditions (25.1% (w/w) at pH 7.4, 47.1% (w/w) at pH 6.0, and 82.6% (w/w) at pH 5.0, respectively). This strongly supports our hypothesis that premature release of the cytotoxic drug during blood circulation is minimal due to the favorable stability of the hydrazone linker at pH 7.4.[25] Consequently, patients are expected to greatly benefit from reduced cardiac side effects because of lower free DOX blood concentrations.[26]

Feasibility of effective tumor targeting and cell killing with this novel, stimulus-induced drug delivery system was assessed using the human MDA-MB-231 breast cell line, which is a generally accepted in vitro model of hormone-independent breast cancer cells overexpressing folate receptors.[27] Drug-containing SJNCs with and without FA targeting ligands were incubated with MDA-MB-231 cells in Hank's balanced salt solution (HBSS), pH 7.4 (for detailed composition see Experimental Section, Supporting Information). After a 4 h incubation period, cells were washed twice with HBSS and incubated another 48 h using serum-containing media before cell viability was quantified. To demonstrate folate-mediated cellular uptake,

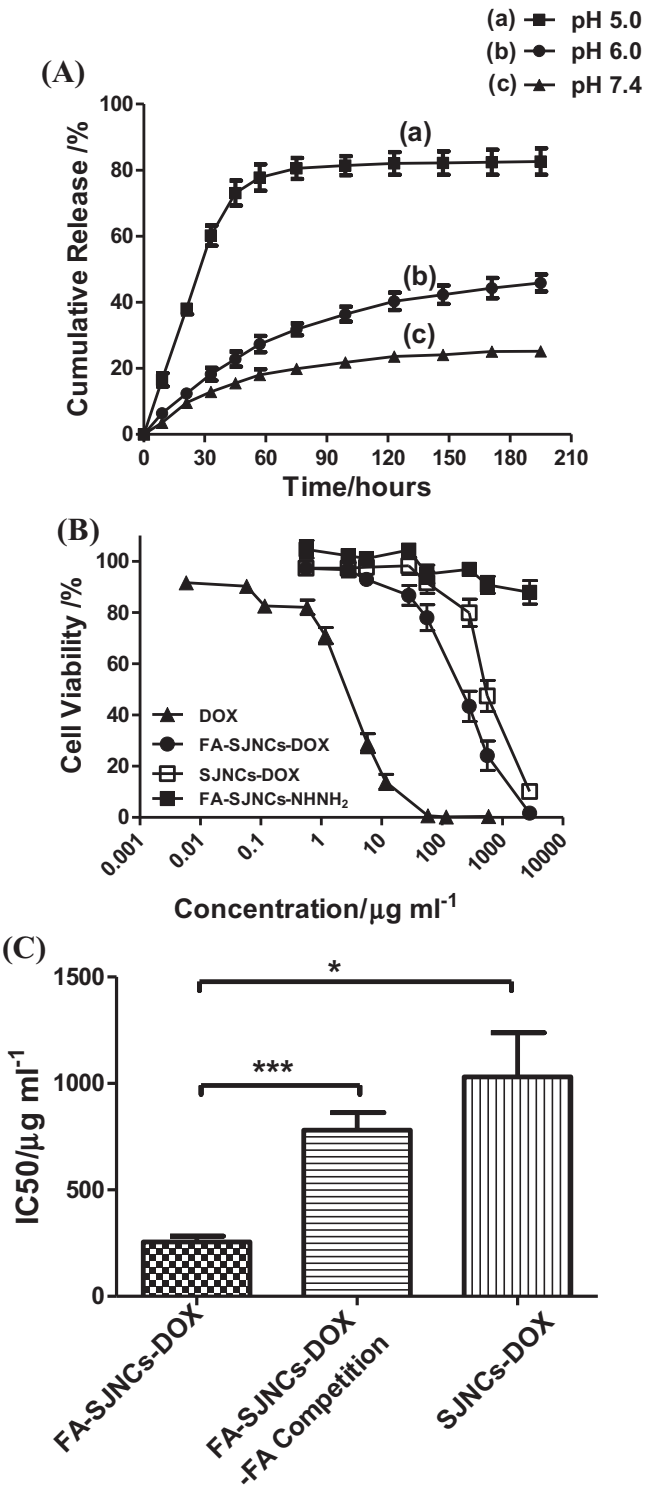

Figure 3. A) DOX release profiles from SJNCs-DOX conjugates at a) pH 5.0; b) pH 6.0, and c) pH 7.4. B) In vitro cytotoxicity profiles of DOX, FA-targeted SJNCs-DOX conjugates, non-targeted SJNCs-DOX conjugates, and drug-free control SJNCs (FA functionalized and hydrazide modified, i.e., FA-SJNCs-$NHNH_2$) using human MDA-MB-231 breast cancer cells. C) IC50 values estimated for FA-targeted SJNCs-DOX in the presence and absence of 1 mM FA and non-targeted SJNCs-DOX (n = 3, $*p < 0.05$, $***p < 0.001$).

competition experiments were performed in the presence of 1 mM FA using the same experimental procedure.

Dose-dependent cytotoxicity profiles for free DOX, DOX-loaded Janus systems, and drug-free control particles are shown in Figure 3B,C. In the absence of drug, Janus particles were reasonably safe up to 3 mg mL^{-1} (cell viability >90%). DOX alone significantly reduced viability of MDA-MB-231 breast cancer cells in a dose-dependent manner. The concentration killing 50% of the cells (IC50) was estimated as 3.3 ± 0.3 μg mL^{-1}. Janus particles with covalently attached DOX (SJNCs-DOX) also reduced cell viability of these human breast cancer cells with an estimated IC50 of 1030.2 ± 416.1 μg mL^{-1}. Since the mechanism of action requires DOX to enter the nucleus, these results suggest that this cytotoxic drug is efficiently released from the Janus structure after cell internalization. Considering an average drug loading efficiency of ≈2% (w/w), the apparent cytotoxicty of DOX coupled to non-targeted Janus particles was five-fold reduced when compared to free DOX. In contrast, FA-targeted drug-containing Janus particles (FA-SJNCs-DOX) were significantly more toxic reducing viability of these breast cancer cells with an IC50 of 255.3 ± 55.1 μg mL^{-1} (see Supporting Information, Table S1). Normalized to the ≈2% (w/w) drug loading efficiency, these results imply an apparent cytotoxicty equivalent to free DOX. To delineate whether folate-mediated endocytosis effectively contributes to the equipotent cytotoxicity of FA-SJNCs-DOX, cell viability studies were performed in the presence of 1 mM FA. Inclusion of this competitor for the folate receptor binding sites is anticipated to dramatically reduce folate-mediated endocytosis of FA-SJNCs-DOX. The four-fold increase in the IC50 for FA-SJNCs-DOX in the presence of 1 mM FA clearly demonstrates that covalent coupling of FA as targeting ligand dramatically augments cellular internalization of this novel nanocomposite resulting in a similar cytotoxicity profile on a per weight basis as free DOX. To further elucidate the impact of the Janus geometry on cellular internalization, computer simulation studies as performed by Ma and colleagues[28] could effectively lead to refined specifications of Janus nanocomposites with increased target selectivity and efficacy.

In summary, a unique Janus assembly was developed comprised of polystyrene/Fe_3O_4@silica. Our experimental data demonstrate that this versatile system possesses dual surfaces for effective conjugation of functionally different chemical moieties. Surface immobilization of FA targeting ligands on the carboxyl-functionalized PS matrix effectively enhances tumor-selective targeting and internalization. Attachment of DOX via a pH-sensitive hydrazone linker to the silica surface enables controlled, stimulus-induced release of the cytotoxic drug after internalization under acidic conditions in endosomal compartments. Silica-embedded Fe_3O_4 nanoparticles render this Janus nanostructure super-paramagnetic suitable for multimodal imaging and hyperthermia-induced sensitization of tumor cells. Consequently, this novel nanoassembly with dual surface functionalities offers an innovative drug delivery platform for multidimensional cancer treatment.

Supporting Information

Supporting Information is available from the Wiley Online Library or from the author.

Acknowledgements

This work was supported by the National Natural Science Foundation of China (No. 51003077, No. 51173135, and No. 51073121), Shanghai Nano-program (No. 11nm0506100), and the Fundamental Research Funds for the Central Universities.

Received: March 27, 2013
Published online: May 16, 2013

[1] C. H. Lee, S. H. Cheng, I. P. Huang, J. S. Souris, C. S. Yang, C. Y. Mou, L. W. Lo, *Angew. Chem. Int. Ed.* **2010**, *49*, 8214.
[2] F. M. Kievit, O. Veiseh, N. Bhattarai, C. Fang, J. W. Gunn, D. Lee, R. G. Ellenbogen, J. M. Olson, M. Q. Zhang, *Adv. Funct. Mater.* **2009**, *19*, 2244.
[3] G. Liu, J. Xie, F. Zhang, Z. Y. Wang, K. Luo, L. Zhu, Q. M. Quan, G. Niu, S. Lee, H. Ai, X. Y. Chen, *Small* **2011**, *7*, 2742.
[4] I. Ojea-Jimenez, L. Garcia-Fernandez, J. Lorenzo, V. F. Puntes, *ACS Nano* **2012**, *6*, 7692.
[5] H. S. Cho, Z. Dong, G. M. Pauletti, J. Zhang, H. Xu, H. Gu, L. Wang, R. C. Ewing, C. Huth, F. Wang, D. Shi, *ACS Nano* **2010**, *4*, 5398.
[6] A. D. Quach, G. Crivat, M. A. Tarr, Z. Rosenzweig, *J. Am. Chem. Soc.* **2011**, *133*, 2028.
[7] a) M. Ferrari, *Nat. Rev. Cancer* **2005**, *5*, 161; b) M. E. Gindy, R. K. Prud'homme, *Expert Opin. Drug Delivery* **2009**, *6*, 865.
[8] J. Hu, S. X. Zhou, Y. Y. Sun, X. S. Fang, L. M. Wu, *Chem. Soc. Rev.* **2012**, *41*, 4356.
[9] S. H. Hu, X. H. Gao, *J. Am. Chem. Soc.* **2010**, *132*, 7234.
[10] a) K. H. Roh, D. C. Martin, J. Lahann, *Nat. Mater.* **2005**, *4*, 759; b) K. H. Roh, M. Yoshida, J. Lahann, *Materialwiss. Werkst.* **2007**, *38*, 1008; c) C. J. Xu, B. D. Wang, S. H. Sun, *J. Am. Chem. Soc.* **2009**, *131*, 4216.
[11] M. Lattuada, T. A. Hatton, *Nano Today* **2011**, *6*, 286.
[12] a) J. R. Howse, R. A. L. Jones, A. J. Ryan, T. Gough, R. Vafabakhsh, R. Golestanian, *Phys. Rev. Lett.* **2007**, *99*; b) Y. Wang, B. H. Guo, X. Wan, J. Xu, X. Wang, Y. P. Zhang, *Polymer* **2009**, *50*, 3361; c) S. Hwang, K. H. Roh, D. W. Lim, G. Y. Wang, C. Uher, J. Lahann, *Phys. Chem. Chem. Phys.* **2010**, *12*, 11894; d) Z. F. Li, D. Y. Lee, M. F. Rubner, R. E. Cohen, *Macromolecules* **2005**, *38*, 7876.
[13] a) T. M. Ruhland, A. H. Groschel, A. Wather, A. H. E. Muller, *Langmuir* **2011**, *27*, 9807; b) S. H. Kim, A. Abbaspourrad, D. A. Weitz, *J. Am. Chem. Soc.* **2011**, *133*, 5516.
[14] a) T. S. Shim, S. H. Kim, J. Y. Sim, J. M. Lim, S. M. Yang, *Adv. Mater.* **2010**, *22*, 4494; b) S. N. Yin, C. F. Wang, Z. Y. Yu, J. Wang, S. S. Liu, S. Chen, *Adv. Mater.* **2011**, *23*, 2915.
[15] Z. W. Seh, S. H. Liu, S. Y. Zhang, M. S. Bharathi, H. Ramanarayan, M. Low, K. W. Shah, Y. W. Zhang, M. Y. Han, *Angew. Chem. Int. Ed.* **2011**, *50*, 10140.
[16] V. Percec, D. A. Wilson, P. Leowanawat, C. J. Wilson, A. D. Hughes, M. S. Kaucher, D. A. Hammer, D. H. Levine, A. J. Kim, F. S. Bates, K. P. Davis, T. P. Lodge, M. L. Klein, R. H. DeVane, E. Aqad, B. M. Rosen, A. O. Argintaru, M. J. Sienkowska, K. Rissanen, S. Nummelin, J. Ropponen, *Science* **2010**, *328*, 1009.
[17] Y. L. Wang, F. Wang, B. D. Chen, H. Xu, D. L. Shi, *Chem. Commun.* **2011**, *47*, 10350.
[18] M. Feyen, C. Weidenthaler, F. Schuth, A. H. Lu, *J. Am. Chem. Soc.* **2010**, *132*, 6791.
[19] a) R. J. Lee, P. S. Low, *Methods Mol. Med.* **2000**, *25*, 69; b) P. S. Low, W. A. Henne, D. D. Doorneweerd, *Acc. Chem. Res.* **2008**, *41*, 120.
[20] H. J. Zhang, C. L. Wang, B. A. Chen, X. M. Wang, *Int. J. Nanomed.* **2012**, *7*, 235.
[21] I. Hilger, W. A. Kaiser, *Nanomedicine* **2012**, *7*, 1443.

[22] Y. L. Wang, H. Xu, Y. S. Ma, F. F. Guo, F. Wang, D. L. Shi, *Langmuir* **2011**, *27*, 7207.
[23] a) D. Cheng, G. B. Hong, W. W. Wang, R. X. Yuan, H. Ai, J. Shen, B. L. Liang, J. M. Gao, X. T. Shuai, *J. Mater. Chem.* **2011**, *21*, 4796; b) S. Mahajan, V. Koul, V. Choudhary, G. Shishodia, A. C. Bharti, *Nanotechnology* **2013**, *24*, 015603.
[24] Q. D. Hu, H. Fan, Y. Ping, W. Q. Liang, G. P. Tang, J. Li, *Chem. Commun.* **2011**, *47*, 5572.
[25] K. Ulbrich, V. Subr, *Adv. Drug Delivery Rev.* **2004**, *56*, 1023.
[26] a) D. Li, J. Tang, C. Wei, J. Guo, S. L. Wang, D. Chaudhary, C. C. Wang, *Small* **2012**, *8*, 2690; b) S. C. Wuang, K. G. Neoh, E. T. Kang, D. E. Leckband, D. W. Pack, *AIChE J.* **2011**, *57*, 1638.
[27] R. Meier, T. D. Henning, S. Boddington, S. Tavri, S. Arora, G. Piontek, M. Rudelius, C. Corot, H. E. Daldrup-Link, *Radiology* **2010**, *255*, 527.
[28] a) K. Yang, Y. Q. Ma, *Nat. Nanotechnol.* **2010**, *5*, 579; b) H. M. Ding, Y. Q. Ma, *Nanoscale* **2012**, *4*, 1116; c) H. M. Ding, W. D. Tian, Y. Q. Ma, *ACS Nano* **2012**, *6*, 1230.